Synthesis and Caracterization of CTO ($CaTiO_3$)

Silva, M. A. S. (Universidade Federal do Ceará – UFC, marceloassilva@yahoo.com.br, R. Tomas Ildefonso, n° 1300, casa 101, Cambeba, CEP: 60822-366, Fortaleza-CE), Fernandes, T. S. M. (UFC); Santiago, A. A. X. (UFC); Sales, J. C. (UVA); Sombra, A. S. B. (UFC).

ABSTRACT

The objective of this work is to study the ceramic material CTO ($CaTiO_3$) by X-Ray Diffraction. The composites of CTO are widely used in dielectric resonators in communication systems. The CTO was prepared by solid state method in a planetary high energy ball milling (Fritsch Pulverisette 5). Stoichiometric quantities of $CaCO_3$ (Aldrich 99%) and TiO_2 (Merck 99%) were dry milled during 4h with a rotational speed of 370 rpm and then calcined at 1000 ºC for 3h. After, the CTO was studied by X-ray diffraction (XRD). The refinament showed that the CTO was formed with 100% mass, the graph of Williamson-Hall showed a homogeneous sample, with a contraction in the crystal lattice and a reasonably small particle size.

Keywords: solid state method, X-ray diffraction, refinament.

INTRODUCTION

In 1900, the rapid growth of technology radios already covered the frequency ranges of HF (High Frequency) and VHF (Very High Frequency). In the mid-40s, the development of radars was already of great interest because it included the detection of aircraft and missiles air systems, air traffic control, airplanes collision avoidance systems, weather prediction, among others. In this period were developed solid state devices of high frequency, microwave integrated circuits, lines of transmission, waveguide components and systems by satellite communications [(1)].

The application of dielectric materials in microwave technology began to progress since then, being primarily used in microwave circuits such as filters, amplifiers and oscillators. Later, the applications in antennas in the 80's made a big

technological leap in telecommunications, satellites and military electronics [2]. Currently, the use of ceramics dielectric revolutionized many industrial sectors of wireless communications, as it reduced costs considerably and sizes of filters, oscillators and antennas. [3].

Ceramics based in materials with a perovskite structure are an important class of electroceramics [4, 5]. The perovskites form a large family of ceramics, whose name derives from the name of the perovskite material, calcium titanate (CaTiO3), and which have similar crystal structures [6]. The CTO can be synthesized by heating a mixture of calcium oxide, calcium carbonate or calcium hydroxide with titanium dioxide at temperatures between 900 and 1350 ° C. Although typically the crystal structure of perovskite is cubic, the CTO can be trigonal or orthorhombic, depending on the synthesis temperature [7]. Through the X-ray diffraction is possible extract information about the structure of the material, where the technique of x-ray diffraction crystalline phase with the Rietveld refinement allows theoretically to confirm the structure and crystallographic information of the sample in powder form [8].

MATERIALS AND METHODS

In this work, samples of $CaTiO_3$ was sintered from powders of $CaCO_3$ (Aldrich 99%), TiO_2 (Merck 99%), using the conventional solid-state reaction method. Oxide and carbonate were weighed and then the mixture was high-energy ball milling during 4h in a planetary ball mill (Fritsch Pulverisette 5). The rotation speed of the disks carrying the sealed vials was 370 rpm. This operation was used to improve the homogeneity of the powder. Then the powder was calcined at 1000 ºC for 3h.

X-ray diffraction

The X-ray powder diffraction profiles of the samples were recorded using a powder X-ray diffractometer system Panalytical, model X´Pert MRD. Powder samples were fixed on a silicon plate with silicon paste. Patterns were collected at laboratory temperature (about 294 K) using Co - Kα radiation, operated at 40kV and 30mA, with five seconds for each step of counting time along angular range 20-60 (2θ). In the present study is adopted the Rietveld's powder structure refinement analysis [9, 10, 11] of X-ray powder diffraction data to obtain the refined structural parameters.

Scherrer equation

The Scherrer equation is currently the most widely used equation to calculate particle size through the FWHM (Full Width at Half Maximum) of diffraction peak, where it has a simplified way to calculate the particle size. For the beam divergence caused by experimental conditions (instrumental factor) of equipment and non-uniformity of particle sizes, which considerably affects the width of the diffraction peaks do not affect the calculations of particle sizes and micro-deformations, it is necessary measure the performance of a standard sample of particles with large sizes and homogeneous [8].

The calculation of particle size, *L*, was made in the program DBWSTool2.3.exe using the Scherrer equation [12],

$$L = \frac{k\lambda}{\beta \cos\theta} \qquad (A)$$

where ***k*** (constant value 1) is the shape coefficient, ***λ*** is the wavelength, ***β*** is the peak full width at half maximum (FWHM) of each phase and θ is the Bragg angle. The parameter ***β*** was corrected for instrumental width using the following equation:

$$\beta = \sqrt{\beta_{exp}^2 - \beta_{inst}^2} \qquad (B)$$

where β_{exp} is the experimental width and β_{inst} instrumental width that are extracted from a sample pattern of LaB_6 [13].

Williamson-Hall equation

Another classical method to obtain quantitative information on particle size and microstrain considering the enlargement of the diffraction peaks is through the Williamson-Hall plot [8].

The Williamson-Hall plot allows us to extract the microstrain through the angular coefficient (slope of the curve), and mean particle size using the linear coefficient (the

intersection of the curve with the ordinate axis), and their homogeneity from the angular width of peak diffraction is represented by the following equation [14]:

$$\frac{\beta \cdot \cos\theta}{\lambda} = \frac{k}{D} + \frac{4\varepsilon}{\lambda}\operatorname{sen}\theta \qquad (C)$$

where ***β*** is the half width of diffraction peak (FWHM), ***λ*** is the wavelenght of x-rays and ***K*** is a constant (value 1) which determines the point in the network reciprocal, ***D*** is the average size of crystallite, ***ε*** is the microstrain.

RESULTS AND DISCUSSIONS

To perform the refinement was used DBWSTools 2.3.exe program and ICSD [Inorganic Cristal Structure Database] [11]. After the refinament, when calculated the particle size by the equations (A) and (B) the DBWSTool2.3.exe program also provided the values necessary to plot the graph FWHM and Williamson-Hall. The XRD pattern of CTO with their refinament and family of crystallographic plans is shown in Fig. 1. It was noted that the sample showed no secondary phases, having formed only $CaTiO_3$ orthorhombic.

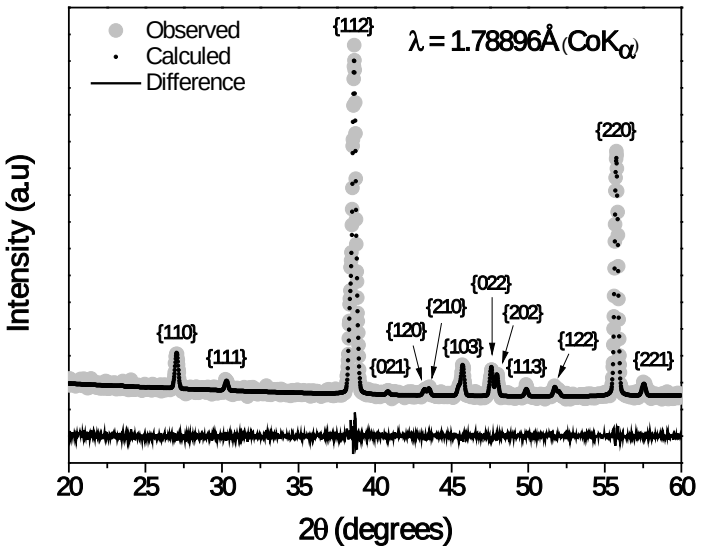

Figure 1. XRD pattern of CTO with their refinament and family of crystallographic plans.

In Table 1 are shown some parameters of the refinament. As the factor R-WP is the most significant statistical factor among all factors which best reflects the progress of refinament, since its analytical expression involves the method of least squares [15], the value found for it was very good because are usually considered satisfactory values between 10-20%. Another factor that presented a satisfactory value was S, being 1 (one) the standard value to classify the refinament as appropriate [11], and in the refinamento of CTO, the value was lower than expected.

Table 1 - Values of some parameters of the refinament for the CTO

% R-WP	% R-EXPECTED	S	% MASS
8.30	10.83	0.76	100

In Table 2 the results of crystallite size are presented by family crystallographic planes and the average of these values. This form of presentation has intention to show the isotropy of the same or not. It is possible to verify a difference in particle size on the crystallographic planes, the value of the average size found showed that the sample has a reasonably small particle size.

Table 2 – Particle size by Scherrer for the CTO

Particle size (nm)	
Family of crystallographic planes {hkl}	
{110}	43.7 (2)
{111}	44.8 (2)
{112}	47.4 (2)
{021}	47.9 (2)
{120}	48.7 (2)
{210}	48.8 (2)
{103}	49.4(2)
{022}	49.9 (2)
{202}	50.0 (2)
{113}	50.4 (2)
{122}	51.0 (2)
{220}	51.7 (2)
{221}	52.1 (2)
Average size	48.9 (2)

The graph FWHM as a function of the angle 2θ is shown in Fig.2, where the particle size does not vary as homogeneous, which was expected, since despite the Scherrer equation be calculeted using the LaB_6 standard sample, it does not take directly into account the microdeformation in their calculations of particle size as the equation of Williamson-Hall.

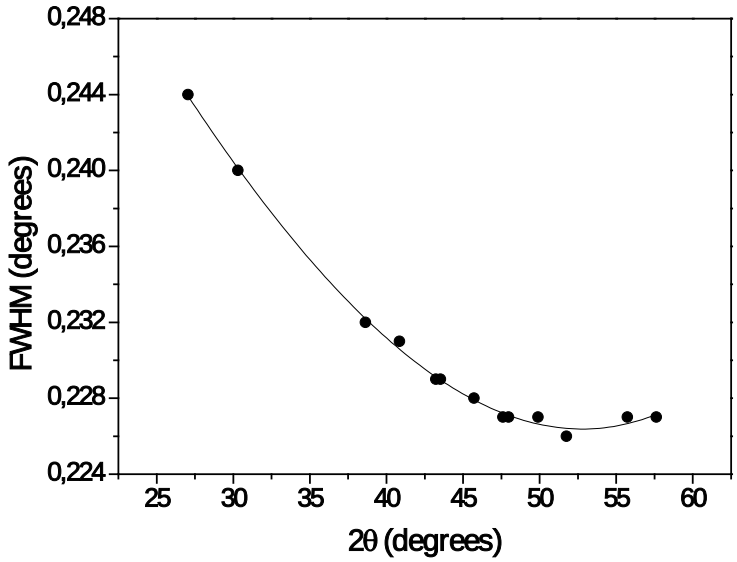

Figure 2. Graph FWHM of CTO as a function of the angle 2θ.

The Fig. 3 show the graph Williamson-Hall as a function of the sen θ, that presents a straight decreasing, indicating a homogeneous sample, but with microstrain negative, representing a contraction in the crystal lattice. Using equation (C) was calculated value of crystallite size and microstrain, respectively by a linear and angular coefficient of straight graph Williamson-Hall.

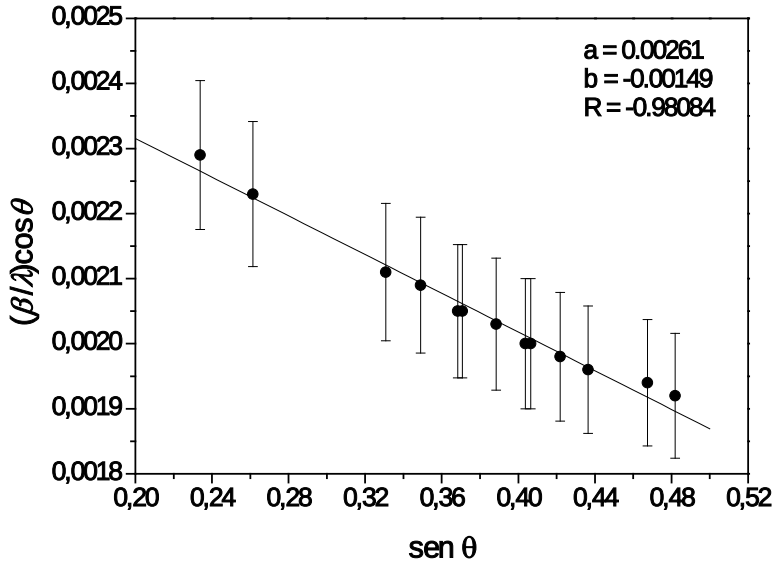

Figure 3. Graph Williamson-Hall of CTO as a function of the sen θ.

In Table 3 can be seen the microstrain and the comparison of the average particle size by Scherrer and Williamson-Hall. The microstrain value is close to zero. This value is much smaller than that for the microstrain value of 0.01% obtained for standard Si powder that is free of any microstrain, indicating that the CTO is not experiencing any microstrain [16]. There is a difference between the values of average particle size obtained by Scherrer and Williamson-Hall. This is because the sample did not show homogeneity, as can be seen in Fig. 2, which presents a parabolic distribution [14].

Table 3 – Microstrain and average particle size by Scherrer and Williamson-Hall

Microstrain (%)	Average particle size (nm)	
	Scherrer	Williamson-Hall
-6.77×10^{-4} (2)	48.9(2)	37.8 (2)

CONCLUSIONS

The refined sample showed R-WP and S satisfactories, where the S value was less than 1 (characteristic of the sample), and R-WP proved to be even better than they normally are considered satisfactory, which is between 10% and 20 %[11]. The Fig. 1 shows that the calculated part was very close to the measured (observed), resulting in a difference of least squares without much variation [10]. Thus, it was confirmed by refinement using DBWSTool2.3.exe that there is only one phase present the $CaTiO_3$ (CTO). The average particle size calculated from Williamson-Hall had a value lower than that calculated by Scherrer. Despite this, the values are considered small. The CTO is not experiencing any microstrain.

ACKNOWLEDGMENTS

CELESTICA, LOCEM, FUNCAP, CAPES, CNPq, X-ray Laboratory (UFC) and the U. S. Air Force Office of Scientific Research - AFOSR (FA9550-08-1-0210).

REFERENCES

(1) POZAR, D. M. ***Microwave Engineering***. 2nd Ed., John Wiley & Sons, Inc., United States of America, 1998.

(2) Kajfez, D., and P. Guillon, (eds.). ***Dielectric Resonators***. Dedham, MA: Artech House, 1986.

(3) SEBASTIAN, M. T. ***Dielectric Materials for wireless Comunication***. Elsevier, Ltd., London, 2008.

(4) LIU, X. M.; FU, S. Y.; HUANG, C. J. Synthesis and magnetic characterization of novel $CoFe_2O_4$ – $BiFeO_3$ nanocomposites. ***Materials Science and Engineering B***. v.121, p. 225-260, 2005.

(5) KIMURA, T., KAWAMOTO, S., YAMADA, I., AZUMA, M., TAKANO, M., TOKURA, Y. ***Physical Review B***, v. 67, 180401, 2003.

(6) GUERRA, J. DE LOS SANTOS. ***Dispersão Dielétrica em Materiais Ferroelétricos***. 2004, 125p. Tese (Doutorado em Física – Física) - Universidade Federal de São Carlos, UFSCar/SP, São Paulo.

(7) CHUNG, C. Y., CHANG, Y. H., CHANG, Y. S., CHEN, G. J. ***Journal of Alloys and Compounds***, 385, 9298, 2004.

(8) MENESES, C. T. ***Estudo da cristalização de nanopartículas de NiO por difração e absorção de raios-X***. 2007, 143p. Tese (Doutorado em Física-Física) - Universidade Federal do Ceará, UFC/CE,Fortaleza.

(9)] Rietveld, H. Line profiles of neutron powder-diffraction peaks for structure refinement. ***Acta Crystallographica,*** v. 22, n. 1, p. 151–152, 1967.

(10) Rietveld, H. A profile refinement method for nuclear and magnetic structures. ***Journal of Applied Crystallography,*** v. 2, n. 2, p. 65–71, 1969.

(11) Young, R. A., Introduction to the Rietveld Method. In:Young, R.A. (ed.). ***The Rietveld Method***. London: Oxford, University Press, 1993.

(12) Williamson, G. K., Hall, W. H., X-Ray line broadening from filed aluminium and wolfram, ***Acta Metallurgica***, 1, p.21-31, 1953.

(13) A. F. L. Almeida, P. B. A. Fechine, M. P. F. Graça, M. A. Valente, A. S. B. Sombra. Structural and Electrical Study of $CaCu_3Ti_4O_{12}$ (CCTO) obtained in a New Ceramic Procedure. ***J Mater Sci***: Mater Electron, 20: p.163-170, 2009.

(14) MEDEIROS, A. M. L. ***Síntese e caracterização de nanopartículas de Cr_2O_3 através do método sol-gel protéico***. 2007, 99p. Dissertação (Mestrado em Engenharia e Ciências de Materiais-Engenharia Metalúrgica) - Universidade Federal do Ceará, UFC/CE,Fortaleza.

(15) PAIVA-SANTOS, C.O. Aplicações do Método Rietveld. ***Instituto de Química da UNESP***, 2001.

(16) RAI, S.K.; KUMAR, A.; SHANKAR, V.; JAYAKUMAR, T; K. RAO, B.S.; RAJ, B. Characterization of microstructures in Inconel 625 using X-ray diffraction peak broadening and lattice parameter measurements. ***Scripta Materialia.*** v. 51, p. 59–63, 2004.